

From pure C₃₆ fullerene to cagelike nanocluster: a density functional study

Shu-Wei Tang · Feng-Di Wang · Yu-Han Li ·
Fang Wang · Shao-Bin Yang · Hao Sun ·
Ying-Fei Chang · Rong-Shun Wang

Received: 29 August 2013 / Accepted: 18 October 2013 / Published online: 22 November 2013
© Springer-Verlag Berlin Heidelberg 2013

Abstract The geometrical structures, energetics properties, and aromaticity of C_{36-n}Si_n ($n \leq 18$) fullerene-based clusters were studied using density functional theory calculations. The geometries of C_{36-n}Si_n clusters undergo strong structural deformation with the increase of Si substitution. For the most energy favorable structures of C_{36-n}Si_n, the silicon and carbon atoms form two distinct homogeneous segregations. Subsequently, the binding energy, HOMO–LUMO energy gap, vertical ionization potential, vertical electron affinity, and chemical hardness for the energetic favorable C_{36-n}Si_n geometries were computed and analyzed. In addition, the aromatic property of C_{36-n}Si_n cagelike clusters was investigated, and the result demonstrate that these C_{36-n}Si_n cagelike structures possess strong aromaticity.

Keywords Density functional study · Fullerene · Nanostructure · Chemical hardness · Nucleus-independent chemical shift

S.-W. Tang · F.-D. Wang · Y.-H. Li · F. Wang · H. Sun ·
Y.-F. Chang (✉) · R.-S. Wang (✉)
Institute of Functional Material Chemistry, Faculty of Chemistry,
Northeast Normal University, Changchun, Jilin 130024, China
e-mail: changyf299@nenu.edu.cn
e-mail: wangrs@nenu.edu.cn

S.-W. Tang
e-mail: tangsw911@nenu.edu.cn

S.-W. Tang · H. Sun · R.-S. Wang
National and Local United Engineering Lab for Power Battery,
Changchun, Jilin 130024, China

S.-B. Yang
School of Material Science and Engineering, Liaoning Technical
University, Fuxin, Liaoning 123000, China

Introduction

Doping fullerene with various elements has attracted intense research efforts since the discovery of C₆₀ [1, 2]. Interest in fullerene-based nanomaterials originates from the diverse dopants and capricious structures, which lead to exceptional physical, chemical and optoelectronic properties with potential applications in material science [3]. In recent years, several doped fullerenes have been produced successfully through introducing different dopants; examples include transition-metal atoms [4], lanthanum and niobium [5], and nitrogen and boron [6–8]. Owing to the good performance of silicon carbide as a tunable bandgap semiconductor with high breakdown field strength, high thermal conductivity, and high saturation drift velocity [3, 9], many studies are searching for C_mSi_n fullerene-based nanostructures [9–13]. Silicon, which has the same kind of outer electronic structure as carbon, is an ideal candidate for C_mSi_n fullerene-like structures. However, Si prefers to form tetrahedral structures because of its *sp*³-like bond features, and substitution of silicon will induce high instability. Therefore, with many Si atoms added, local strains increase in magnitude. Nevertheless, some experimental and theoretical studies have explicitly proved the existence of Si-doped heterofullerenes [14–23]. Ray et al. [10] acquired significant evidence of C_{2n-q}Si_q ($2n = 32–100$; $q < 4$) cage-type clusters via mass spectroscopy experiments. Moreover, a series of attempts was made to acquire C_{60-n}Si_n ($n \leq 30$) cagelike clusters [16–24]. Nevertheless, other than the experimental and theoretical studies on C_{60-n}Si_n cagelike clusters, few works on silicon substituted small fullerenes have been reported [25–28]. The interesting issue with silicon heterofullerenes is to know to what extent carbon atoms can be substituted without destroying the cage framework, and to reveal the arrangement of silicon atoms in cagelike clusters, as well as the electronic and aromatic properties caused by Si substitution. However, due to the low chemical stability of

small fullerenes, theoretical investigations on small C_mSi_n cage-like clusters are so far scarce.

Considering the absence of small C_mSi_n fullerene-like nanostructures, carbon fullerenes are usually considered as model structures. Among the numerous small carbon fullerenes, C_{36} is one of the “magic-number” fullerenes that has gained special attention [29, 30]. Nevertheless, few experimental works have been reported on C_{36} exclusively. Nuclear magnetic resonance spectra indicate that C_{36} fullerene has a D_{6h} point group [31]. Subsequent theoretical calculation showed that another D_{2d} C_{36} isomer exists that is almost isoenergetic to the D_{6h} structure [32, 33]. By virtue of the D_{6h} and D_{2d} isomers having a minimal number of adjacent pentagons, they are expected to be candidates for C_{36} fullerene. In the present work, we performed a density functional theory (DFT) study on the structural, energetic, and aromatic properties of $C_{36-n}Si_n$ fullerene-based materials. Our results not only deepen understanding of the growth mechanism of C_mSi_n -based nanostructures and size-dependent evolution of physical properties, but will also inspire further experimental study to synthesize these novel fullerene-like materials.

Computational methodology

All calculations were performed with the Gaussian 09 quantum chemical package [34]. Geometry optimizations were carried out without any symmetry constraints using the B3LYP functional [35, 36] in combination with the 6-31G(d) basis set. The accuracy of the B3LYP/6-31G(d) method has been proved acceptable for geometry optimization of large molecules [37, 38]. To make sure that the obtained lowest-energy structures are real local minima, normal-mode vibrational analysis was applied. All the energy minima obtained for the lowest-energy $C_{36-n}Si_n$ clusters were confirmed by the absence of an imaginary mode. The electronic properties of the $C_{36-n}Si_n$ clusters were analyzed on geometrical structures obtained at the B3LYP/6-31G(d) level. Vertical ionization potentials (VIP) and vertical electron affinities (VEA) were calculated as the total energy differences between clusters and charged clusters with the assumption that the electron transfer occurred in a time too short for the cluster to respond. In addition, aromaticity of $C_{36-n}Si_n$ cage-like clusters was evaluated by calculating nucleus-independent chemical shifts (NICS) [39, 40] at the molecule's center using the gauge-including-atomic-orbital (GIAO) method at B3LYP/6-31G(d) level.

Results and discussion

Geometrical structures of $C_{36-n}Si_n$

In the book *An Atlas of Fullerenes* [41], among all the 15 mathematically possible conventional isomers for C_{36}

fullerene, only the D_{6h} and D_{2d} isomers have the minimal count of 12 pentagon adjacencies. According to the pentagon adjacency penalty rule (PAPR) [42], the most stable structure should be the one with the smallest number of adjacent pentagons. Consequently, the D_{6h} and D_{2d} C_{36} cages are predicted to be most stable, and their geometrical structures are presented in Fig. 1. D_{6h} C_{36} has a geometrical structure of a highly symmetric spheroid, with six-membered cyclic polyacene, joined to hexagonal terminal caps. For D_{2d} C_{36} , eight hexagons are divided into two separate tetracene-like subunits by a chain made up of 12 pentagons.

To study $C_{36-n}Si_n$ cage-like clusters, the first challenge is to find the lowest energy favorable structures. On the basis of D_{6h} and D_{2d} C_{36} cages, $C_{36-n}Si_n$ clusters were obtained in the following way (as suggested by Huda et al. [9]). Firstly, a Si atom is placed arbitrarily at a substitutional site in D_{6h} C_{36} fullerene and the energy favorable structure obtained through comparing different symmetry nonequivalent sites. Next, a second Si atom is introduced in all symmetrically distinguishable positions of the most stable $C_{35}Si$ structures to obtain a $C_{34}Si_2$ cluster. From $C_{34}Si_2$, the other energetically favorable structures of $C_{33}Si_3$, $C_{32}Si_4$, . . . are achieved in a similar way. The methodology of Si substitution for D_{2d} C_{36} fullerene was similar. Previous studies have proved that C_mSi_n clusters with equal proportions of silicon and carbon atoms are particularly stable, and the substitutional C_mSi_n clusters become unstable as the number of silicon atoms increases [43].

The energy favorable structures of $C_{36-n}Si_n$ ($n=1-18$) cage-like clusters proceeding from D_{6h} and D_{2d} C_{36} fullerene are presented in Tables 1 and 2. In these systems, the structures of clusters are distorted and yet maintained, and structural deformation occurred mainly in the vicinity of Si atoms. In the clusters from D_{6h} C_{36} fullerene, the $C_{35}Si$ has a framework in which a Si atom locates at the fusion site of a pair of pentagons and hexagons. The distance from Si to the cage center is 3.572 Å, about 0.880 Å longer than that of carbon atoms at the equivalent site, thus the Si atom tends to emerge from the cage structure. Mulliken charge analysis shows that an evident charge transfer exists between Si and C atoms. The Si atom in $C_{35}Si$ has a positive charge of 0.352 $|e|$, and, accordingly, a negative charge is distributed uniformly among its first carbon neighbor atoms, as can be expected from

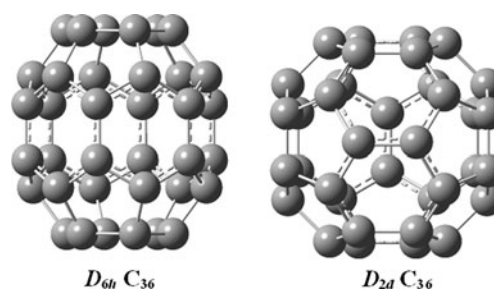


Fig. 1 Structures of C_{36} (D_{6h} and D_{2d}) fullerene

Table 1 The lowest-lying cage-like structures obtained by substituting D_{6h} C_{36} fullerene


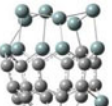
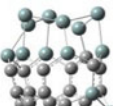
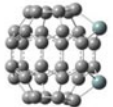
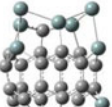
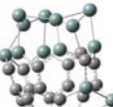
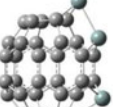
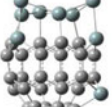
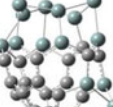
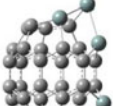
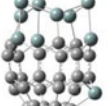
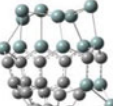
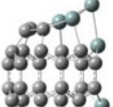
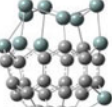
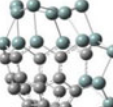
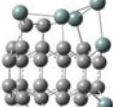
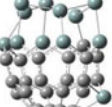
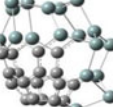


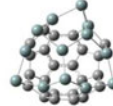

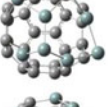
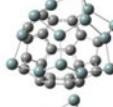


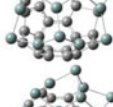
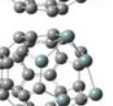
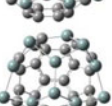

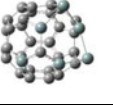
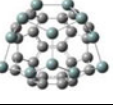
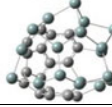



No.	State	E_b (eV/atom)	Structure	No.	State	E_b (eV/atom)	Structure	No.	State	E_b (eV/atom)	Structure
1	$^1A'$	8.43		7	1A	7.76		13	1A	7.06	
2	1A	8.32		8	1A	7.65		14	1A	6.95	
3	1A	8.19		9	1A	7.54		15	1A	6.84	
4	1A	8.08		10	1A	7.42		16	1A	6.73	
5	1A	7.97		11	1A	7.31		17	1A	6.62	
6	1A	7.87		12	1A	7.18		18	1A	6.51	

Table 2 The lowest-lying cage-like structures obtained by substituting D_{2d} C_{36} fullerene

No.	State	E_b (eV/atom)	Structure	No.	Sym.	E_b (eV/atom)	Structure	No.	Sym.	E_b (eV/atom)	Structure
1	1A	8.44		7	1A	7.77		13	1A	7.10	
2	1A	8.32		8	1A	7.66		14	1A	6.99	
3	1A	8.21		9	1A	7.55		15	1A	6.88	
4	1A	8.10		10	1A	7.44		16	1A	6.77	
5	1A	7.97		11	1A	7.33		17	1A	6.66	
6	1A	7.87		12	1A	7.21		18	1A	6.55	

electronegativity considerations [44]. As an inference, the C–Si bonds are partially ionic. With Si substitution, the structural transition from $C_{35}Si$ to $C_{34}Si_2$ is very symmetrical. Two Si atoms in the $C_{34}Si_2$ cluster occupy the para position of the hexagon, and the Si–Si bond is 3.329 Å. Next, as with $C_{33}Si_3$, a contorted cage structure with Si atoms standing in line is proposed to be the most energetically favorable. The Si–Si bond is 2.334 Å, which is comparable to the bond distance in bulk silicon (2.345 Å). Starting from $C_{32}Si_4$, the Si atom show a tendency to assemble, and this evolutionary trend continues up to the $C_{18}Si_{18}$ cluster. Considering that the Si atom prefers to be accommodated in sp^3 bonding hybridization, another configuration corresponding to spatially separated sets will lead to a decrease in stability. As a consequence, not only is there a structural deformation in the vicinity of Si atoms but a segregation of Si and C atoms in $C_{36-n}Si_n$ cluster also clearly stands out. Accordingly, the segregation pattern increases in extent as the silicon content increases.

For the lowest-lying $C_{35}Si$ configuration from $D_{2d} C_{36}$ fullerene, the Si atom sits at the junction between a pair of pentagons and a hexagon. The Si–C bonds range from 1.938 Å to 1.954 Å, compared to the bonds of Si_nC_n ($n=10–15$) clusters [28]. In the $C_{34}Si_2$ cluster, two Si atoms present a symmetrical distribution, with a Si–Si distance of 3.316 Å, slightly shorter than that of replacing $D_{6h} C_{36}$ via Si substitution. For production of $C_{33}Si_3$, the third Si atom prefers to locate beside the existing Si atom, just as in $C_{33}Si_3$ from the $D_{6h} C_{36}$ cage. Nevertheless, an obvious difference also exists between these two types of $C_{36-n}Si_n$ cage-like clusters, viz., the Si atoms herd together from $n=4$ for Si substitutions in the $D_{2d} C_{36}$ cage rather than $n=18$ for the $D_{6h} C_{36}$ cage. Consequently, both C and Si atoms tend to form subunits spontaneously in the $C_{31}Si_5–C_{18}Si_{18}$ cluster structures.

After presenting the low-lying structures, it is very interesting to discuss the structural properties of $C_{36-n}Si_n$ ($n=1–18$) clusters. The average bond lengths, and Mayer bond orders of C–C, Si–C, and Si–Si bonds are given in Table 3. Along with the longer length in going from C–C to Si–Si bonds, the relative chemical bonds strength decreases in the order C–C > Si–C > Si–Si. The bond lengths show significant variation with respect to the type of C–C, Si–C, Si–Si bonds in $C_{36-n}Si_n$ clusters. The corresponding average distances of C–C, Si–C, Si–Si bonds in the cage-like clusters from the $D_{6h} C_{36}$ cage vary in the range of 1.434–1.455 Å, 1.821–1.914 Å, and 2.334–2.418 Å, respectively; and the counterparts of cage-like clusters from $D_{2d} C_{36}$ cage range from 1.433–1.442 Å for C–C bonds, 1.852–2.015 Å for Si–C bonds, and 2.344–2.458 Å for Si–Si bonds, respectively. By virtue of the structural distortion caused by C–C, Si–C, and Si–Si bonds, there is a tendency to maximize the number of C–C and Si–C bonds to relieve the strain energy. As a consequence, the Si atoms prefer to “pop out” in all $C_{36-n}Si_n$ ($n=1–18$) clusters, similar to the case of small nonstoichiometric C_mSi_n clusters [19–23].

Table 3 also lists the average Mayer bond orders of C–C, Si–C, Si–Si bonds, which are proportional to the bond strength between different atoms [45]. For D_{6h} and $D_{2d} C_{36}$ cages, the average bond orders for C–C bonds are 1.226 and 1.229, which is comparable to the predicted bond order (1.250) of C–C bonds in C_{60} . These results also lie between the values of the single bond in ethane (1.02) and the double bond in ethene (1.75) [46]. For Si–C bonds, the bond orders range from 0.882 to 1.122 for cage-like clusters deriving from $D_{6h} C_{36}$ cage, and 0.840–1.075 for those cage-like clusters from $D_{2d} C_{36}$ cage, respectively, approaching 0.953 in silacyclobutane [47]. Due to the large distances in Si–Si bonds, a variety of average bond orders with considerably smaller values are observed. The smallest value reaches 0.733 for the $C_{32}Si_4$ cluster from the $D_{6h} C_{36}$ cage and 0.702 for the $C_{33}Si_3$ cluster from the $D_{2d} C_{36}$ cage.

Stabilities and energetic properties

The stability of $C_{36-n}Si_n$ cage-like clusters is still an intractable issue since no experimental confirmation has been reported. The binding energy (E_b) is known to be an important quantity for estimating stability and possibility for experimental synthesis of $C_{36-n}Si_n$ cage-like clusters; E_b can be calculated according to following equation:

$$E_b(C_{36-n}Si_n) = \frac{1}{36}[(36-n)E(C) + nE(Si) - E(C_{36-n}Si_n)] \quad (1)$$

where $E(X)$ is the total energy of the corresponding X system. The binding energies for the lowest-energy structures of $C_{36-n}Si_n$ clusters are also tabulated in Tables 1 and 2. The E_b for $C_{36-n}Si_n$ clusters decreases with silicon substitution. Accordingly, a structure with one Si substitution is the most energetically favorable, and isomers where the C–Si proportion equals 1:1 are found to be less stable energetically. The E_b values of the $C_{35}Si$ system are 8.43 and 8.44 eV/atom, respectively, i.e., about 0.12 eV and 0.13 eV/atom smaller than those of pristine D_{6h} and $D_{2d} C_{36}$ fullerene. Furthermore, a monotonically decreasing relationship between binding energy and the concentration of silicon is also observed from Tables 1 and 2; therefore, silicon substitution costs almost the same amount of energy (about 0.12 eV) despite the number of carbon atoms that have been replaced before.

Additionally, the energy gap (E_{gap}) between the highest occupied molecular orbital (HOMO) and the lowest molecular orbital (LUMO) is also an important factor influencing the structural stability. The E_{gap} values for D_{6h} and $D_{2d} C_{36}$ fullerene are 1.09 and 1.39 eV, respectively, i.e., about 38.7 % and 21.9 % smaller than that of C_{60} [48]. Looking at Fig. 2a, a significant oscillation is observed in the evolution trend of the E_{gap} with respect to silicon content. For clusters from $D_{6h} C_{36}$ fullerene, the E_{gap} of $C_{28}Si_8$ is particularly

Table 3 Average bond lengths (Å) and average Mayer bond order (in parenthesis) of Si–Si, Si–C, and C–C bonds

Molecule	D_{6h}			D_{2d}		
	C–C	Si–C	Si–Si	C–C	Si–C	Si–Si
C ₃₆	1.442 (1.226)			1.442 (1.229)		
C ₃₅ Si ₁	1.441 (1.231)	1.905 (0.882)		1.440 (1.943)	1.943 (0.840)	
C ₃₄ Si ₂	1.438 (1.242)	1.909 (0.885)		1.438 (1.243)	1.921 (0.864)	
C ₃₃ Si ₃	1.439 (1.234)	1.930 (0.885)	2.334 (0.779)	1.438 (1.240)	1.835 (1.011)	2.458 (0.702)
C ₃₂ Si ₄	1.438 (1.236)	1.914 (0.903)	2.400 (0.733)	1.440 (1.234)	2.015 (0.929)	2.401 (0.729)
C ₃₁ Si ₅	1.437 (1.237)	1.906 (0.917)	2.418 (0.734)	1.441 (1.231)	1.972 (0.995)	2.400 (0.779)
C ₃₀ Si ₆	1.436 (1.237)	1.918 (0.890)	2.391 (0.739)	1.441 (1.234)	1.854 (1.056)	2.349 (0.857)
C ₂₉ Si ₇	1.436 (1.239)	1.900 (0.923)	2.394 (0.748)	1.441 (1.232)	1.872 (1.026)	2.119 (0.989)
C ₂₈ Si ₈	1.434 (1.243)	1.883 (1.041)	2.410 (0.738)	1.437 (1.240)	1.907 (0.946)	2.344 (0.859)
C ₂₇ Si ₉	1.434 (1.244)	1.903 (0.911)	2.370 (0.763)	1.438 (1.240)	1.873 (1.001)	2.357 (0.853)
C ₂₆ Si ₁₀	1.434 (1.247)	1.887 (0.946)	2.381 (0.757)	1.439 (1.236)	1.854 (1.058)	2.363 (0.861)
C ₂₅ Si ₁₁	1.435 (1.245)	1.868 (1.089)	2.376 (0.759)	1.439 (1.232)	1.868 (1.015)	2.358 (0.860)
C ₂₄ Si ₁₂	1.436 (1.243)	1.854 (1.034)	2.373 (0.771)	1.440 (1.192)	1.852 (1.075)	2.363 (0.835)
C ₂₃ Si ₁₃	1.438 (1.235)	1.850 (1.061)	2.362 (0.775)	1.438 (1.236)	1.867 (1.008)	2.363 (0.816)
C ₂₂ Si ₁₄	1.438 (1.238)	1.845 (1.067)	2.373 (0.762)	1.437 (1.229)	1.888 (0.960)	2.361 (0.807)
C ₂₁ Si ₁₅	1.439 (1.236)	1.831 (1.091)	2.376 (0.759)	1.435 (1.240)	1.880 (0.964)	2.367 (0.795)
C ₂₀ Si ₁₆	1.439 (1.231)	1.821 (1.122)	2.375 (0.768)	1.436 (1.238)	1.856 (1.018)	2.370 (0.800)
C ₁₉ Si ₁₇	1.455 (1.230)	1.826 (1.107)	2.365 (0.794)	1.433 (1.238)	1.885 (0.956)	2.360 (0.801)
C ₁₈ Si ₁₈	1.439 (1.227)	1.827 (1.111)	2.360 (0.805)	1.433 (1.241)	1.868 (0.991)	2.360 (0.789)

large, whereas C₂₅Si₁₁ has the smallest value of 0.83 eV. As for clusters from D_{6h} C₃₆ fullerene, the C₂₁Si₁₅ and C₃₄Si₂ clusters have the largest and smallest value of E_{gap} , respectively. Nevertheless, the E_{gap} for all C_{36-n}Si_n cage-like clusters is not very large, and varies from 0.83 to 1.35 eV for clusters from the D_{6h} C₃₆ cage, and 1.07 to 1.60 eV for those from the D_{2d} C₃₆ cage, respectively. Thus, these clusters are expected to be very reactive. Figure 2a also shows that E_{gap} for clusters from the D_{2d} cage are notably larger than those values of C_{36-n}Si_n clusters from the D_{6h} cage overall, except in the case of C₃₄Si₂ and C₂₈Si₈ clusters. Consequently, the C_{36-n}Si_n cage-like clusters from the D_{2d} cage are more stable in energy.

The vertical electron affinity (VEA, energy difference between the neutral and mono-anionic molecules on the basis of the same neutral geometry) and vertical ionization potential (VIP, energy difference between the monocationic and the neutral molecule based on the same neutral geometry) are also important parameters for estimating the stability of C_{36-n}Si_n clusters. Figure 2b and c present VIPs and VEAs of C_{36-n}Si_n cage-like structures. The VIP value of D_{6h} C₃₆ fullerene is 6.61 eV, about 2.1 % greater than those of D_{2d} C₃₆ cage. Nevertheless, these two C₃₆ isomers possess smaller VIPs in comparison with C₆₀ (7.05 V) and, consequently, D_{6h} and D_{2d} C₃₆ fullerenes are liable to lose electrons. In view of the overall situation, the evolutionary trend of VIPs is quite similar to the case of the HOMO–LUMO gap. This downward trend gives an indication that the reactivity of pure D_{6h} and

D_{2d} C₃₆ fullerene increases as the silicon increases. Except for C₃₄Si₂, clusters from the D_{2d} C₃₆ cage have a larger VIP with respect to the VIP of D_{6h} C₃₆ fullerene, implying that it is difficult to remove electrons from these clusters. For VEA values, there is no notable separation region between the cage-like clusters from D_{6h} and D_{2d} C₃₆ fullerene. The C_{36-n}Si_n cage-like structures have higher VEA values than the D_{2d} and D_{6h} cage on the whole (the VEA for D_{2d} and D_{6h} fullerene are 2.16 and 2.57 eV, respectively), and therefore these clusters have a slightly more reactive nature. Hence, this may be one reason that the C_{36-n}Si_n clusters have not been observed in experimental studies until now.

On the basis of the VIP and the VEA, the global chemical hardness (η) [49] can be approximated by following formula:

$$\eta \approx \frac{1}{2}(\text{VIP} - \text{VEA}) \quad (2)$$

As is well known, cluster structures with large hardness values are often considered to be hard, and thus less reactive or more stable. Figure 2d offers a graphic definition of chemical hardness for all C_{36-n}Si_n cage-like clusters. The C₃₃Si₃ clusters in both D_{2d} and D_{6h} fullerene have the highest values of chemical inertness (2.13 and 1.96 eV, respectively), implying that these two clusters are relatively stable among C_{36-n}Si_n clusters. Other clusters with apparent low values of chemical hardness may present an obstacle to finding these

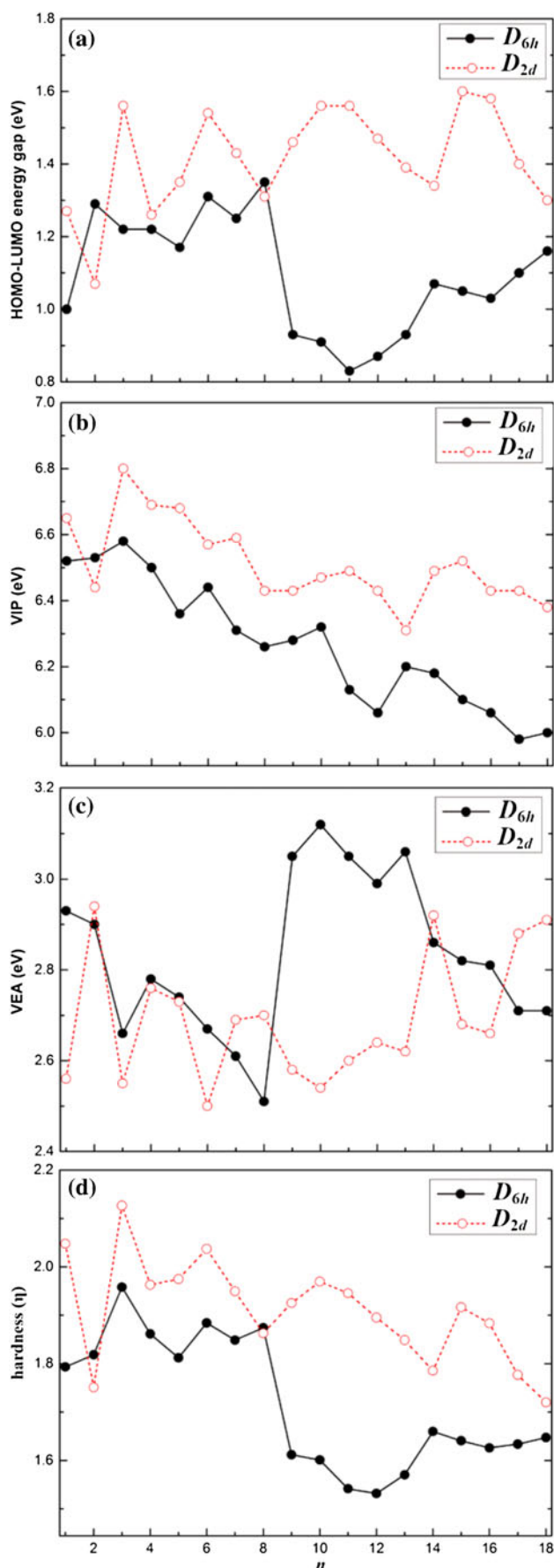


Fig. 2 Size dependence of **a** the HOMO–LUMO energy gap, **b** vertical ionization potential (VIP), **c** vertical electron affinity (VEA), and **d** chemical hardness (η) of $C_{36-n}Si_n$ clusters ($n=1-18$). The characteristic values of clusters from D_{2d} and D_{6h} C_{36} fullerene are represented by a dashed line/open circles and solid line/filled circles, respectively

experimentally. The evolutionary tendency of chemical hardness is in good agreement with the HOMO–LUMO gap, and accordingly, an empirical correlation between the chemical hardness and HOMO–LUMO gap can be established qualitatively, viz., a hard molecule usually has a large HOMO–LUMO gap, and a soft molecule possesses a small HOMO–LUMO gap.

Aromatic stabilization energies

With respect to the stability of cage-like compounds, aromatic stabilization energies can provide some useful hints. The nucleus-independent chemical shift (NICS) technique is the most common magnetic index of aromaticity in cage structure despite the existence of some flaws and limitations [50–54]. Previous study shows that aromatic molecules are chemically more stable than less aromatic or antiaromatic molecules [49]. In general, aromaticity and antiaromaticity are characterized by negative and positive NICS values, respectively. The NICS values of the $C_{36-n}Si_n$ clusters are presented in Fig. 3. The NICS values of pristine D_{6h} and D_{2d} C_{36} fullerene obtained at B3LYP/6-31G(d) level are -27.08 and -11.20 ppm, respectively, i.e., more negative than that of C_{60} [-4.25 ppm at B3LYP/6-311G(d) level]; these cages therefore present a strong aromatic character. With silicon substitution, the delocalized π electrons of the carbon cage are broken and then rebuilt on the remaining carbon subunit of the cage. In $C_{36-n}Si_n$ clusters, the Si has a stronger preference for sp^3 hybridization, and therefore Si substitution leads to a severe change of delocalized π electrons, as evidenced by the NICS

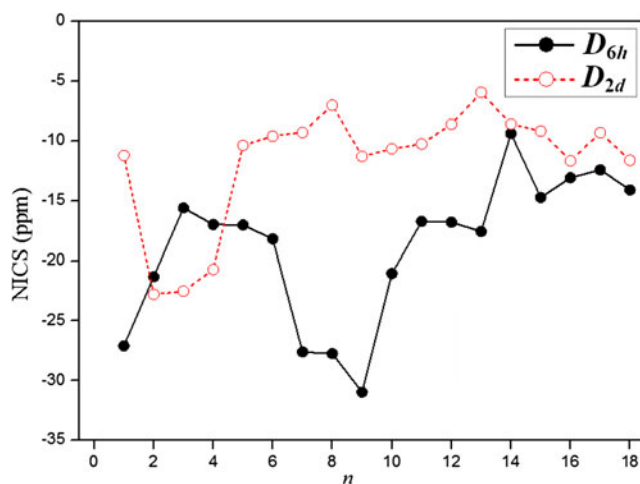


Fig. 3 Nucleus-independent chemical shift (NICS) values versus Si content in $C_{36-n}Si_n$ ($n=0-18$) clusters

value at the cage center. The NICS values range from -9.37 to -30.95 ppm for clusters from the D_{6h} C_{36} cage and -5.92 to -22.77 ppm for those from the D_{2d} C_{36} cage, respectively. As to the set of clusters deriving from the D_{6h} C_{36} cage, only $C_{30}Si_6$, $C_{29}Si_7$, and $C_{28}Si_8$ clusters present more negative values than their parent C_{36} fullerene, and therefore these clusters shows an increase in aromaticity. Furthermore, it is also interesting to compare the NICS of cagelike clusters from the D_{2d} C_{36} cage with the corresponding values from the D_{6h} C_{36} cage. As Fig. 3 shows, compared to the NICS of cagelike clusters from the D_{6h} C_{36} cage, the $C_{35}Si$, $C_{34}Si_2$, and $C_{33}Si_3$ from D_{2d} C_{36} cage have more negative NICS values, indicating stronger aromatic properties. The NICS values become less negative with further Si substitution, especially for $C_{24}Si_{12}$ (NICS: -5.92 ppm), presenting weak aromaticity. The reason may be attributed to fact that, in the $C_{36-n}Si_n$ clusters, carbon atoms preserve the conjugated pattern of fullerene while Si–Si bonds create a perturbing network capping the cluster. Consequently, these $C_{36-n}Si_n$ heterofullerenes yield less negative NICS values at their cage centers. In addition, it is very interesting to compare the evolutionary trend of aromaticity with that of chemical hardness. As showed in Fig. 2d and Fig. 3, a parallel exists between aromaticity and chemical hardness in $C_{36-n}Si_n$ heterofullerenes, i.e., the $C_{36-n}Si_n$ cluster with the more negative NICS value is often a hard molecule, while counterparts with less negative or positive NICS values are soft molecules. For instance, the $C_{28}Si_8$ cluster derived from the D_{6h} C_{36} cage shows the most negative NICS value and a relatively high value of hardness. Therefore, chemical hardness can be served as a qualitative technique to measure aromaticity of $C_{36-n}Si_n$ heterofullerenes, which accords well with the argument of Zhou and Parr [55].

Conclusions

DFT calculations were performed on the low-energy structures of $C_{36-n}Si_n$ ($n \leq 18$) clusters to investigate the effect of silicon doping on the structural relaxation, energetics properties, and aromatic character of C_{36} (D_{6h} and D_{2d}) fullerene. Si substitution brings a new family of $C_{36-n}Si_n$ ($n \leq 18$) clusters. Regarding structural features, a distinct segregation between the silicon and carbon atoms develops as a consequence of aggregation of Si atoms. A significant electron transfer from silicon to carbon atoms was seen in all $C_{36-n}Si_n$ clusters, rendering a partially ionic character to the Si–C bonds. The stability of $C_{36-n}Si_n$ clusters was found to be associated with the silicon content, and binding energies decreased gradually in a linear trend. The cagelike structures from D_{2d} fullerene were more energetically favourable than those from the D_{6h} cage. The E_{gap} , VIP and VEA showed strong variation with respect to Si substitution, and the magnitude of the energy gaps varied from 0.83 to 1.60 eV. Si substitution leads to

negative NICS in $C_{36-n}Si_n$ ($n \leq 18$) clusters, providing an indication of strong aromatic character.

Acknowledgments Financial support from the National Natural Science Foundation of China (Grant No. 51203016 and No. 51274119) and the Fundamental Research Funds for the Central Universities (Grant No. 11QNJJ016) is gratefully acknowledged. The authors also appreciate the invaluable comments and good suggestions from the reviewers.

References

- Kroto HW, Heath JR, O'Brien SC, Curl RF, Smalley RE (1985) *Nature* 318:162–163
- Krätschmer W, Lamb LD, Fostiropoulos K, Huffman DR (1990) *Nature* 347:354–358
- Mélinon P, Masenelli B, Tourmus F, Perez A (2007) *Nat Mater* 6:479–490
- Branz W, Billas IML, Malinowski N, Tast F, Heinebrodt M, Martin TP (1998) *J Chem Phys* 109:3425–3430
- Clemmer DE, Hunter JM, Shelimov KB, Jarrold MF (1994) *Nature* 372:248–250
- Yu R, Zhan M, Cheng D, Yang S, Liu Z, Zheng L (1995) *J Phys Chem* 99:1818–1819
- Guo T, Jin C, Smalley RE (1991) *J Chem Phys* 95:4948–4950
- Wang SH, Chen F, Fann YC, Kashani M, Malaty M, Jansen SA (1995) *J Phys Chem* 99:6801–6807
- Huda MN, Ray AK (2008) *Chem Phys Lett* 457:124–129
- Ray C, Pellarin M, Lermé JL, Vialle JL, Broyer M, Blase X, Mélinon P, Kéghélian P, Perez A (1998) *Phys Rev Lett* 80:5365–5368
- Fye JL, Jarrold MF (1997) *J Phys Chem* 101:1836–1840
- Pellarin M, Ray C, Lermé J, Vialle JL, Broyer M, Blase X, Kéghélian P, Mélinon P, Perez A (1999) *J Chem Phys* 110:6927–6938
- Pellarin M, Ray C, Lermé J, Vialle JL, Broyer M, Blase X, Kéghélian P, Mélinon P, Perez A (1999) *Eur Phys J D* 9:49–54
- Matsubara M, Massobrio C (2005) *J Phys Chem A* 109:4415–4418
- Matsubara M, Massobrio C (2005) *J Chem Phys* 122:084304-1–084304-7
- Matsubara M, Kortus J, Parlebas JC, Massobrio C (2006) *Phys Rev Lett* 96:155502-1–155502-4
- Matsubara M, Massobrio C (2007) *Appl Phys A* 86:289–292
- Matsubara M, Massobrio C (2007) *Solid State Phenom* 129:95–103
- Marcos PA, Alonso JA, Molina LM, Rubio A, López MJ (2003) *J Chem Phys* 119:1127–1135
- Scipioni R, Matsubara M, Ruiz E, Massobrio C, Boero M (2011) *Chem Phys Lett* 510:14–17
- Fu CC, Weissmann M, Machado M, Ordejón P (2001) *Phys Rev B* 63:085411-1–085411-9
- Marcos PA, Alonso JA, López MJ (2005) *J Chem Phys* 123:204323-1–204323-8
- Sprinivasan A, Huda MN, Ray AK (2006) *Eur Phys J D* 39:227–236
- Cheng WD, Wu DS, Zhang H, Chen DG, Wang HX (2002) *Phys Rev B* 66:085422-1–085422-10
- Koponen L, Puska MJ, Nieminen RM (2008) *J Chem Phys* 128:154307-1–154307-7
- Li J, Xia Y, Zhao M, Liu X, Song C, Li L, Li F (2008) *J Chem Phys* 128:154719-1–154719-8
- Wang R, Zhang D, Liu C (2005) *Chem Phys Lett* 411:333–338
- Song B, Yong Y, He P (2010) *Eur Phys J D* 59:399–406
- Kroto HW (1987) *Nature* 329:529–531
- Rohlfing EA, Cox DM, Kaldor A (1984) *J Chem Phys* 81:3322–3330
- Piskoti C, Yarger J, Zettl A (1998) *Nature* 393:771–774

32. Grossman JC, Cote M, Louie SG, Cohen ML (1998) *Chem Phys Lett* 284:344–349
33. Côté M, Grossman JC, Cohen ML, Louie SG (1998) *Phys Rev Lett* 81:697–700
34. Gaussian 09, Revision A.2, Frisch MJ, Trucks GW, Schlegel HB et al (2009) Gaussian, Inc., Wallingford CT
35. Becke AD (1993) *J Chem Phys* 98:5648–5652
36. Lee CT, Yang WT, Parr RG (1998) *Phys Rev B* 37:785–789
37. Tang SW, Feng JD, Qiu YQ, Sun H, Wang FD, Chang YF, Wang RS (2010) *J Comput Chem* 31:2650–2657
38. Tang SW, Sun LL, Feng JD, Sun H, Wang RS, Chang YF (2009) *Eur Phys J D* 53:197–204
39. Schleyer PR, Maerker C, Dransfeld A, Jiao H, Hommes NJRE (1996) *J Am Chem Soc* 118:6317–6318
40. Chen Z, Wannere CS, Corminboeuf C, Puchta R, Schleyer PR (2005) *Chem Rev* 105:3842–3888
41. Fowler PW, Manolopoulos DE (1995) *An atlas of fullerenes*. Oxford University Press, New York
42. Campbell EEB, Fowler PW, Mitchell D, Zerbetto F (1996) *Chem Phys Lett* 250:544–548
43. Pradhan P, Ray AK (2005) *J Mol Struct THEOCHEM* 716:109–130
44. Martínez-Guajardo G, Gómez-Saldival Z, Jana DF, Calaminici P, Corminboeuf C, Merino G (2011) *Phys Chem Chem Phys* 13:20615–20619
45. Pettifor D (1995) *Bonding and structure of molecules and solids*. Clarendon, Oxford
46. Emri J (2003) *J Mol Struct THEO CHEM* 620:283–290
47. Gordon MS, Barton TJ, Nakano H (1997) *J Am Chem Soc* 119:11966–11973
48. Lu X, Chen ZF, Thiel W, Schleyer PR, Huang RB, Zheng LS (2004) *J Am Chem Soc* 126:14871–14878
49. Parr RG, Pearson RG (1983) *J Am Chem Soc* 105:7512–7516
50. An W, Shao N, Bulusu S, Zeng XC (2008) *J Chem Phys* 128:084301-1–085411-9
51. Feixas F, Matito E, Poater J, Solà M (2007) *J Phys Chem A* 111:4513–4521
52. Torres JJ, Islas R, Osorio E, Harrison JG, Tiznado W, Merino G (2013) *J Phys Chem A* 117:5529–5533
53. Lazzeretti P (2000) *Prog Nucl Magn Reson Spectrosc* 36:1–88
54. Islas R, Martínez-Guajardo G, Jiménez-Halla JOC, Solà M, Merino G (2010) *J Chem Theory Comput* 6:1131–1135
55. Zhou Z, Parr RG (1989) *J Am Chem Soc* 111:7371–7379